The effect of slope errors on the performance of the UCB/UCSF – HHMI beamlines

H. A. Padmore Feb 21st, 2000

1. Introduction

The UCB / UCSF – HHMI beamlines have previously been examined for two optical arrangements, one involving sagittal focusing with a mirror and one with a crystal. The assumption has been made previously that it is desirable to keep the imaging distance of the final focusing element as small as possible to reduce the effect of slope errors on image quality. This in turn is limited by the need on the one hand to maximize the flux through a 100μm collimator in a horizontal convergence of 3 mrads, and on the other to keep the vertical demagnification as small as possible, in order to have as small a divergence as possible, to reduce the vertical beam size on the detector to as small a value as possible.

The question addressed here is whether the assumption above is correct, that in order to reduce the effect of slope errors it is desirable to reduce the imaging distance (either by making the whole optical system smaller or by making the demagnification higher). This in turn leads to predictions of slope error tolerances for each element.

2. Simulation of slope errors

The assumption used before was based on the thin lens approximation for a parabolic focusing element. This shows us that if we illuminate a parabolic surface with parallel light, and then rotate the incoming ray directions around a remote fixed point (for example an upstream focusing element), then the image at the nominal gaussian image plane will move by the product of the focal length of the element and the angular deviation. The general scheme under consideration is shown in Fig. 1. It is self evident from simple lens theory that this true, but using the geometry shown in Fig. 2 this will be shown to be true. Point O is the center of a downstream element that can rotate to direct a ray to A or B, for example through a slope error or $\varphi/2$. We therefore have,

$$\theta_2 = 2\theta_1 + \phi$$

$$\theta_1 = \theta - p/R = \theta - \frac{L\phi}{R\theta}$$

$$\theta_2 - 2\theta_1 = \phi - \frac{2L\phi}{R\theta}$$

using the paraxial focusing equation with an object distance of infinity, ie. we are dealing with a parabola in this case, therefore $R\theta = 2r'$. We can then express the deviation of the ray at the image plane as the sum of the displacement at the origin (1st term), and that resulting from the angular separation of the rays from A and B, ie.

$$dy = L\phi + r'\ \phi - \frac{L\phi}{r'} = r'\phi$$

The deviation of the ray in the image plane is therefore the product of the angular deviation of the incoming ray and the imaging distance of the parabolic mirror. In the above derivation we have ignored the very small difference in the position of B relative to A perpendicular to the surface as we are dealing with large radii and small anglular deviations.

We can now compare this result to raytracing results as a check on more complicated geometries. Fig. 3 shows the results from a system employing a parabolic collimating mirror, flat crystal, sagittally curved crystal, and parabolic refocusing mirror, with 2:1 demagnification in the horizontal direction, and 1.23 magnification in the vertical direction. In this geometry we are using an M1 – source distance of 6.5 m, an M2 to image distance of 8 m, and with 20 and 10 m object and image distance respectively for the sagittally focusing crystal. This geometry gives the same magnifications as the 2:1 focusing toroidal mirror scheme previously studied. The image size produced is 47 (v) by 116 (h) μm FWHM. The horizontal image is aberration free, but in the vertical direction the image is a little bigger than the aberration free image size of 29 μm. The simulation was done for a superbend source (5T), 1.9 GeV storage ring energy, and for a photon energy of 12 keV, with rms source sizes of 10 (v) and 100 (h) μm. Fig. 4 shows the same configuration, but with a point source, and this shows an image size of around 5 μm FWHM in the horizontal direction, but a coma like aberration in the vertical direction, with a small single sided core and a full width (FWZH) of the most aberrated rays of 45 μm. Fig. 5 shows the same case with the sagittally focusing crystal C2 rotated by 20 μrads. The image has now been displaced by 330 μm in the vertical direction, and the image has changed shape to be more symmetric in the vertical direction, with a size of around 40 μm FWHM. Fig. 6 shows the same system but with C2 in its un-rotated position, but with M1 rotated by the same amount, 20 μrads. Again we see that the image has been displaced by around 330 μm, and is rather similar in shape and size to the case where C2 is rotated by this amount.

The amount we expect to see the image move by is simply the product of the angular deviation and the image distance of the M2 mirror, ie. 40 μrads x 8 m = 320 μm. The angular deviation of 40 μrads is given by twice the rotation angle. We can see this is rather close to what we observe. Also we can see that the rotation can occur anywhere in the optical system, with similar effect, even though the source of the angular deviation differs by 16 m in the two cases given above.

We now will look at the effect of errors in the sagittal direction, by rolling the optical elements, ie. rotation about an axis in the plane of incidence on the surface of the element. In this case we have to take account of the grazing incidence angle, and the fact that we have a finite object distance. The effect of roll is to rotate the beam at a distance d from the element by the roll angle φ on a radius of $d\sin\theta$, where θ in this case is the grazing incidence angle, ie for small angles we get a translation by an amount $\varphi d \sin\theta$. As the system images from a real object to image plane in the horizontal direction, we have to take account of the magnification. The effect in the image plane is therefore,

$$dx = 2DM\phi\sin\theta$$

where D is the source – element distance, M is the horizontal magnification, φ is the roll angle, and θ is the angle of grazing incidence.

Fig. 7 shows the case where the C1 plane crystal is rolled by 0.01 degrees. According to the above argument the image should translate by 2 x 20 x 0.5 x sin(0.01) sin(9.4) for 12 keV = 0.57 mm, in accord with the simulation. Fig. 8 shows the effect of rolling the M1 premirror by 1 degree. According to the above relation the translation should be 2 x 6.5 x 0.5 x sin(1) x 0.004 = 0.45 mm, again in accord with the simulation. In the case of rolling C1, the image quality was unchanged as expected. However rolling M1 causes significant degradation in the image quality in the vertical direction, with the separation of the most aberrated rays now being 0.25 mm. This reduction in image quality is important for alignment, but not for specifying the sagittal slope error, as these are typically many orders of magnitude lower than the value used here.

The case of the sagittal focusing crystal design was used to illustrate these points as the image is almost aberration free. We will now look at the case of the scheme using toroidal mirror focusing, ie. parabolic collimating mirror (6.5 m from the source, 4 mrads grazing angle), 2 flat crystals (Si[111], 12 keV), and a toroidal mirror (21 m from the souce, 10.5 m from the image plane, 4 mrads grazing angle, focusing from infinity in the vertical direction and from the real source in the horizontal direction; horizontal acceptance 1.5 mrads). Fig. 9 shows the image of a point source, and it can be seen that there is an intense core region in the horizontal direction with small wings, and in the vertical direction a coma-like tail extending to around 60 μm. Fig. 10 shows the same system but with the 2nd crystal, C2, rotated by 20 μrads. The effect is to translate the image in the vertical direction by 0.42 mm (to the sharp leading edge), and to defocus the beam to around 0.2 mm in the horizontal direction. The vertical coma tail is a little larger at around 80 μm FWZH. The displacement of 0.42 mm is expected from the rotation of C2. Using the arguments before, the image should be displaced in the vertical direction by 2 x 20 μrad x 10.5 (10.5 being the M2 – image plane distance in m) = 0.42 mm as observed. The defocusing in the horizontal direction is cause by the fact that unlike the tangential case, the sagittal radius of the mirror is fixed, and so as the C2 crystal is rotated, the sagittal focal length of the mirror changes as the angle of the principal ray changes. This is shown in Fig. 11, where the focal plane is moved downstream by 0.12 m, and clearly the image has moved back into focus in the horizontal direction. Finally, the M1 mirror pitch was changed by 20 μrads, with the rest of the elements in their nominally correct position. The image is shown in Fig. 12 at the gaussian image plane, and it can be seen that as expected it is essentially identical to the same pitch error introduced into C2.

3. **Error budget**

Having established the effect of slope errors, we can now assign a slope error budget to each element. The grazing angle of incidence used in studying the optical systems has changed during the design process, and here we use the latest value of 4.5 mrads. The aberration limited image size for the 2:1 horizontally demagnifying toroidal mirror focusing scheme has previously been established to be 60 (v) x 150 (h) μm FWHM, with an image distance from M2 to the focus of 10.5 m. If we use the rule that the slope error contribution is equal to the above image sizes, leading therefore to a 1.41 increase in image size, then assuming that all 4 elements combine equally as a vector sum, then the slope error

image size for each element would be 30 (v) x 75 (h) μm FWHM. Taking into account angle doubling on reflection, and the 10.5 m image distance of M2, the tangential slope error budget for each element is therefore **1.4 μrads FWHM (0.6 μrads rms)**. The sagittal slope error for M1 and M2 are almost irrelevant, due to the effect of the small grazing angle, and the larger size of the image in this direction. Applying the rules established above, the sagittal slope errors are **2.5 and 7.5 mrads** FWHM respectively for M1 and M2. The sagittal slope error for C1 and C2 crystals is **25 μrads FWHM** (for 12 keV).

4. Comparison with a sagittal focusing crystal design

Finally we should note how the toroidal mirror focusing scheme compares to what would be possible using a sagittal crystal focusing design. In the standard sagital focusing scheme originally studied, the M1 – source distance was 6.5 m, and the M2 – image plane was 3.25 m, ie. 2:1 demagnification. Applying the rules as described before this means that the tangential slope errors can be relaxed by a factor of 3.2, ie. to 4.5 μrads FWHM (1.9 μrads rms).

The advantage of the sagittal focusing scheme is that we can use a small M2 image distances, and hence the required slope error tolerance is larger than in the mirror focusing scheme by a factor of 3.2. This brings the tangential slope error tolerance for all components from the rather challenging value of 0.6 μrad rms, to a more reasonable value of **1.9 μrads rms**. However the disadvantage of the sagittal focusing scheme is the difficulty of the sagittal bending mechanism, the dynamic bending requirement during MAD scans, and (for the 2:1 tangential demagnification case) the greater vertical divergence. The vertical divergence at 2:1 vertical demagnification would be around 0.8 mrads FWHM, and so is probably small enough for all practical cases. In examining the difficulty of each focusing scheme, we therefore have to balance the difficult of the mechanical bending system for the sagittal crystal with the difficulty of achieving the very challenging slope error tolerance in the toroidal mirror scheme.

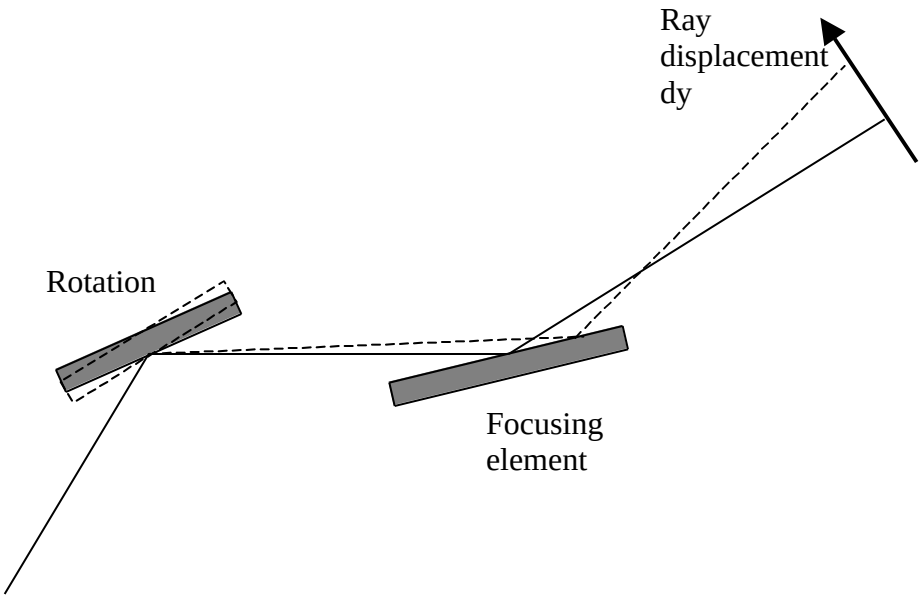

Fig. 1. Rotation of the incoming rays causes a shift in the ray position in the gaussian image plane

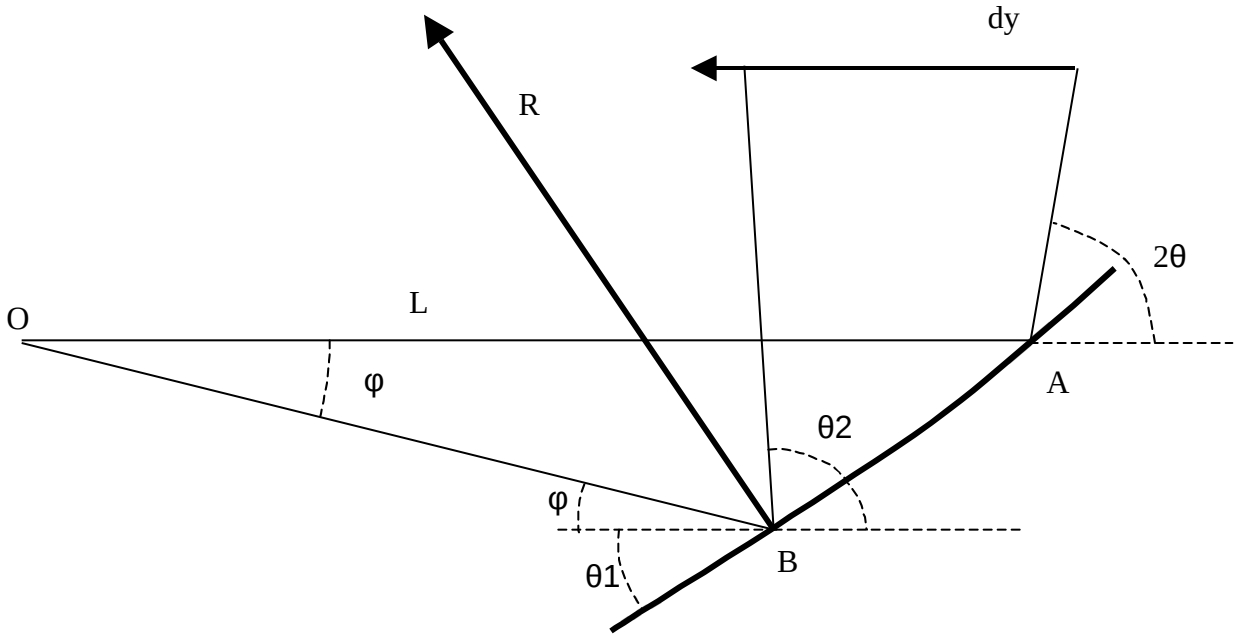

Fig. 2. Geometry for reflection of a ray on a curved surface

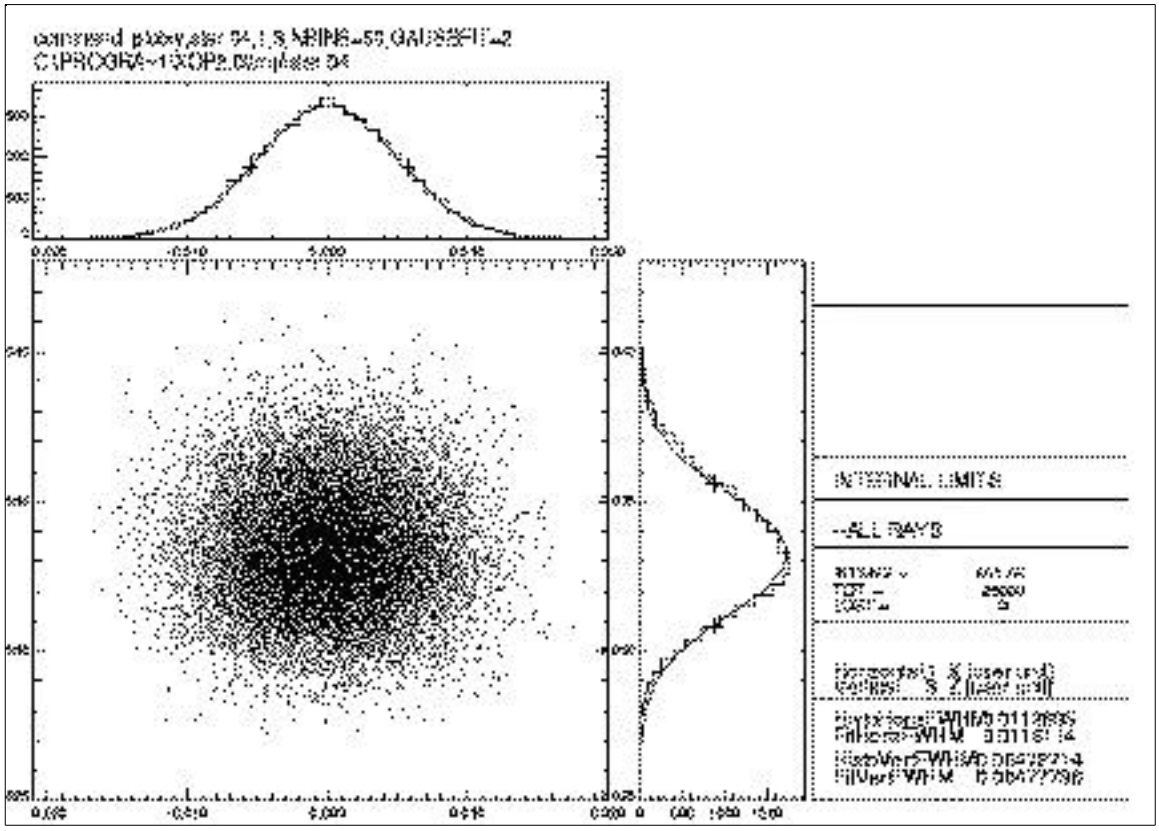

Fig. 3 Image at the focus of a system comprising parabolic collimating mirror, flat crystal, sagittally focusing crystal, and parabolic focusing mirror. The source acceptance is 1.5 mrads, and the system has 2:1 demagnification in each plane. The source – M1 distance is 6.5 m, the M1 – C1 distance is 13.3 m, the C1 – C2 distance is 0.2 m, the C2 – M2 distance is 2 m and the M2 to image plane distance is 8 m. The source dimensions used were 24 and 235 μm FWHM in the vertical and horizontal planes respectively, and the image size is 47 (v) by 116 (h) μm FWHM.

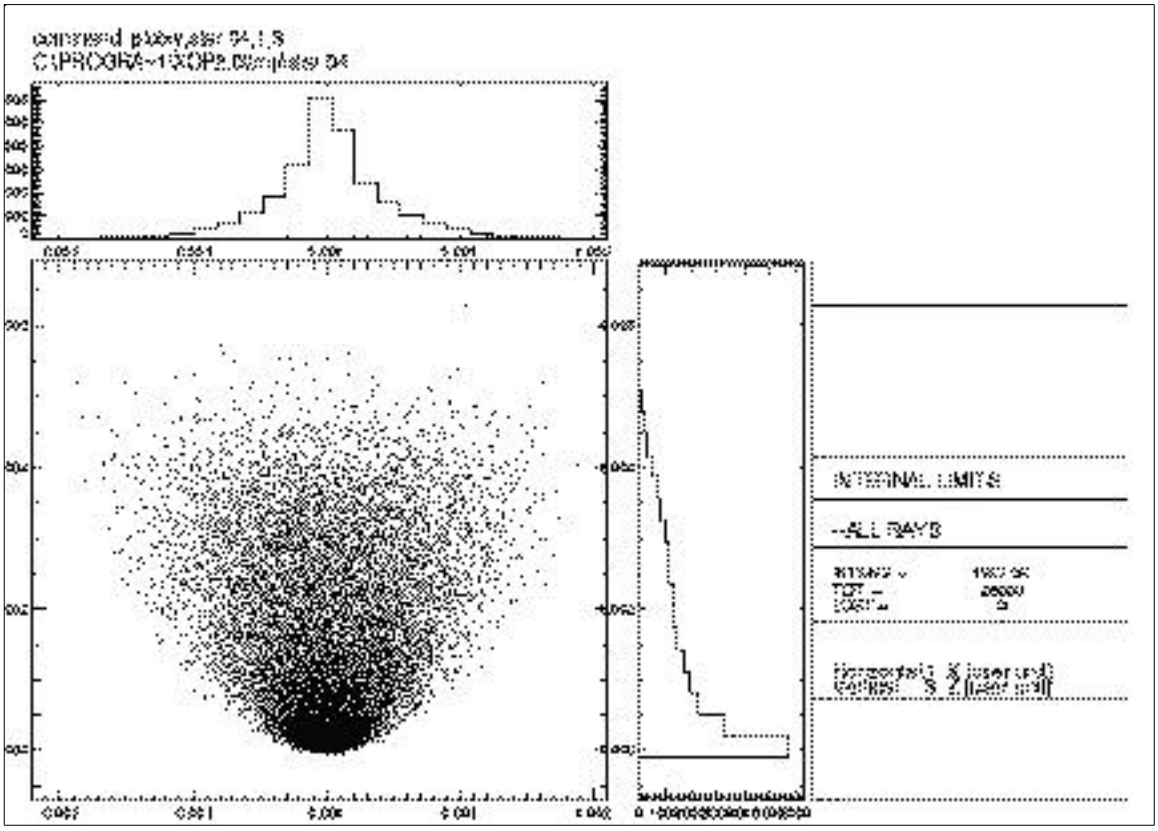

Fig. 4. Image from the system as given in Fig. 3, but with a point source.

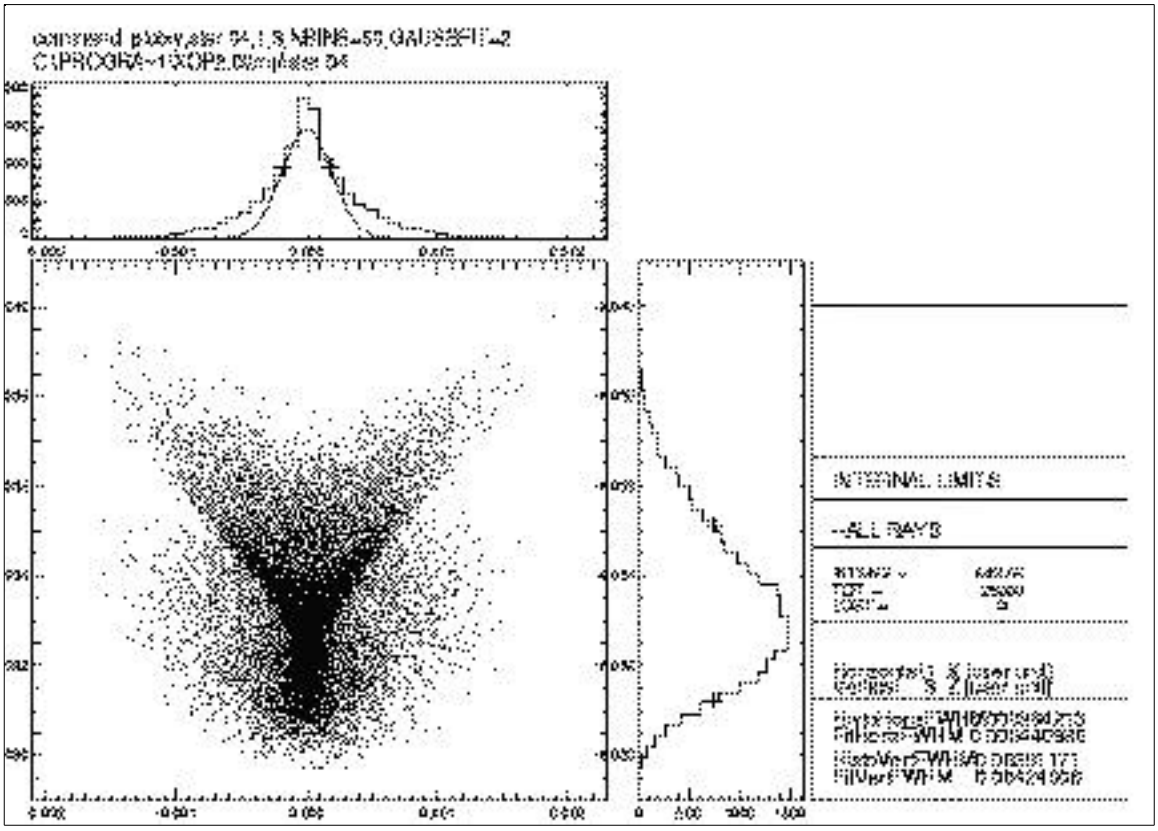

Fig. 5 Image from the same system as given in Fig.3, but for a point source, and for a rotation of the C2 crystal by 20 μrads in pitch. Note that the image core has been displaced vertically by 330 μm, and has a vertical size of 40 μm FWHM.

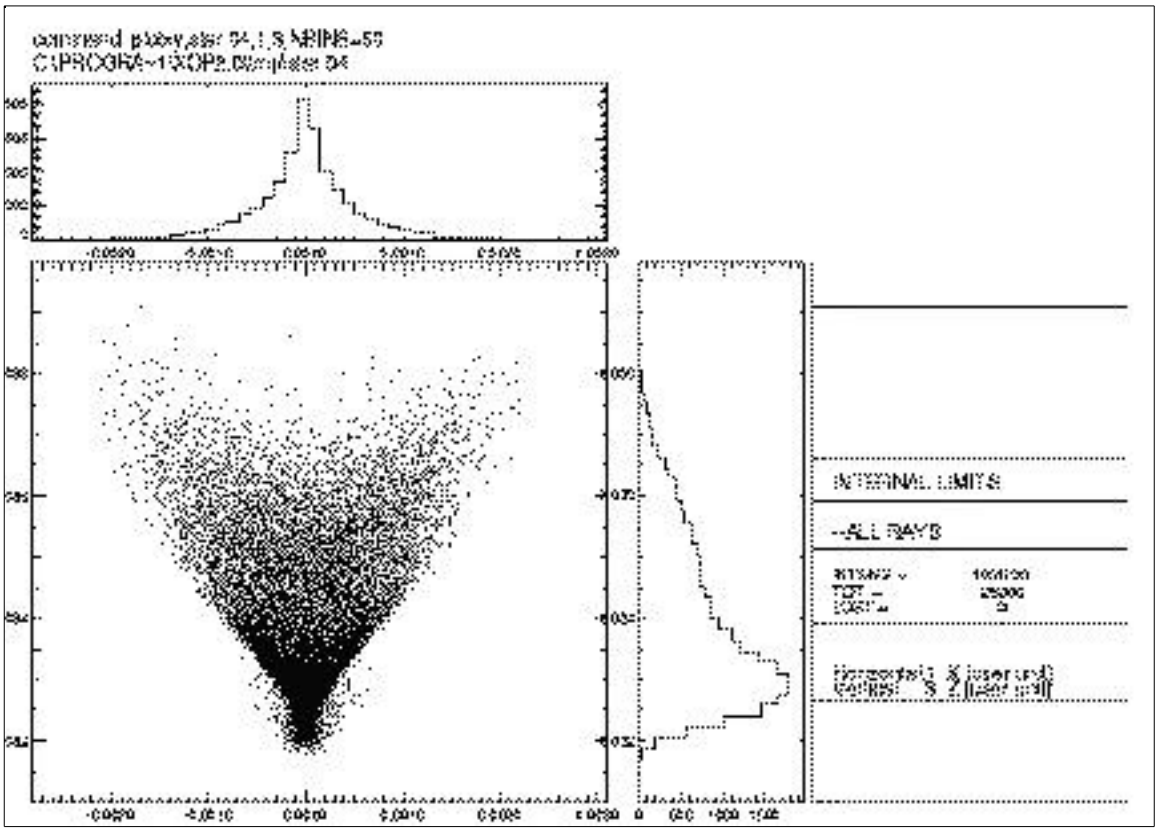

Fig. 6 Image from the same system as given in Fig.3, but for a point source, and for a rotation of the M1 mirror by 20 μrads in pitch. Note that the image core has been displaced vertically by 330 μm, and has a vertical size of 20 μm FWHM for the core, and around 60 μm FWZH (full width zero height, ie. the difference in position of the most aberrated rays).

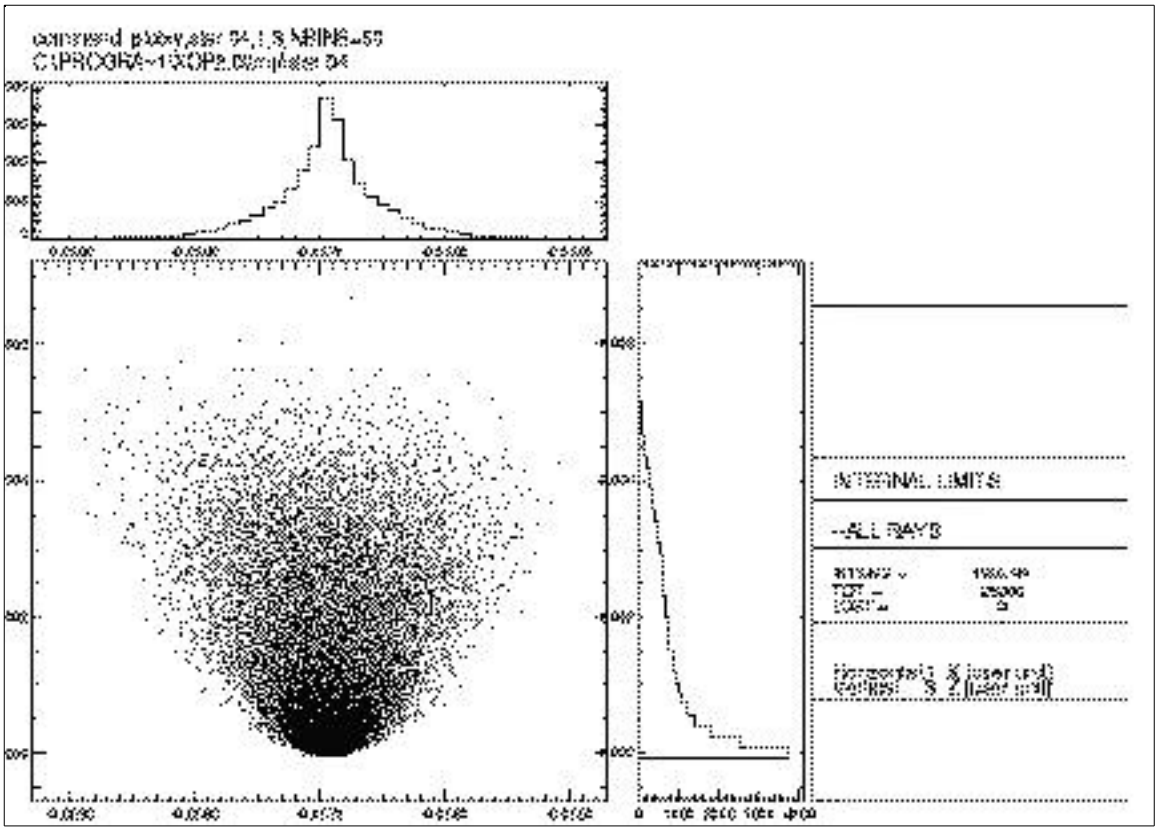

Fig. 7. Image from the same system as given in Fig. 3, with a point source, no tangential pitch error on M1 or C2, but with the 1st crystal C1 rolled by 0.01 degrees. The image has translated in the horizontal direction by 0.57 mm.

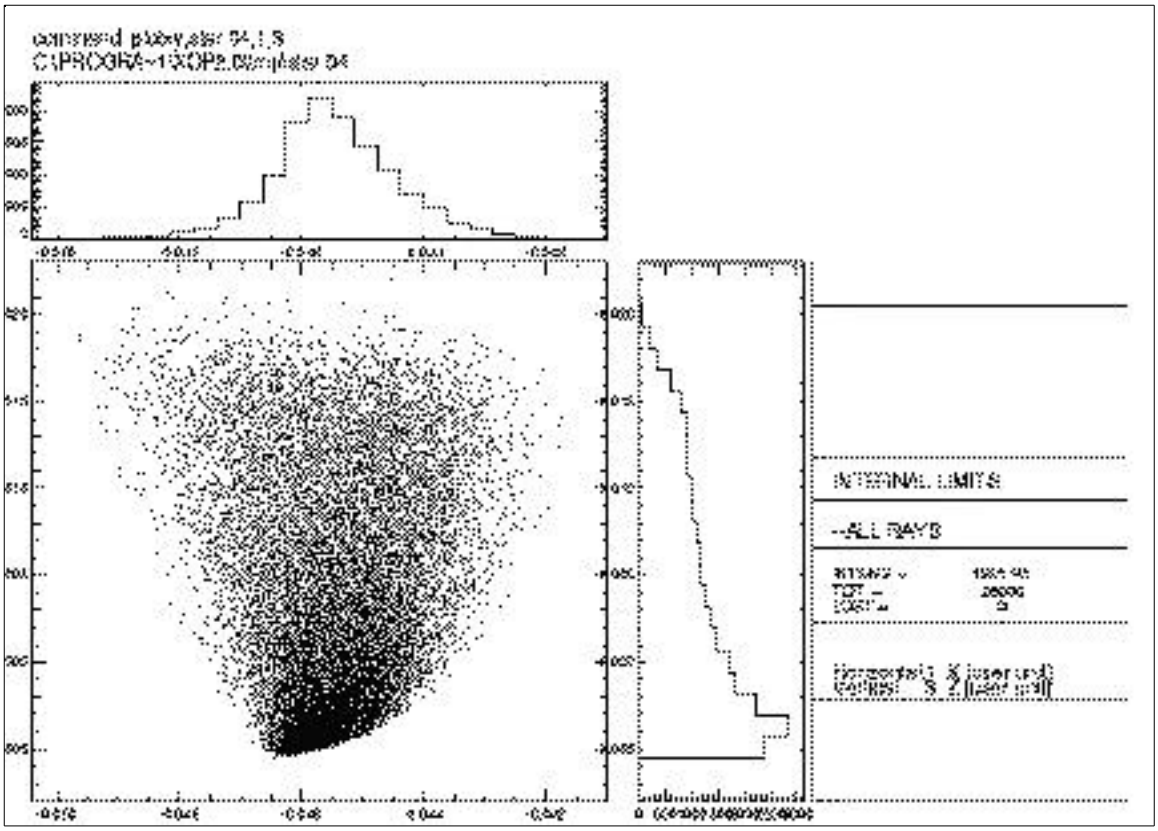

Fig. 8. Image from the same system as given in Fig. 3, with a point source, no tangential pitch error on M1 or C2, but with the M1 mirror rolled by 1 degree. The image has translated in the horizontal direction by 0.46 mm.

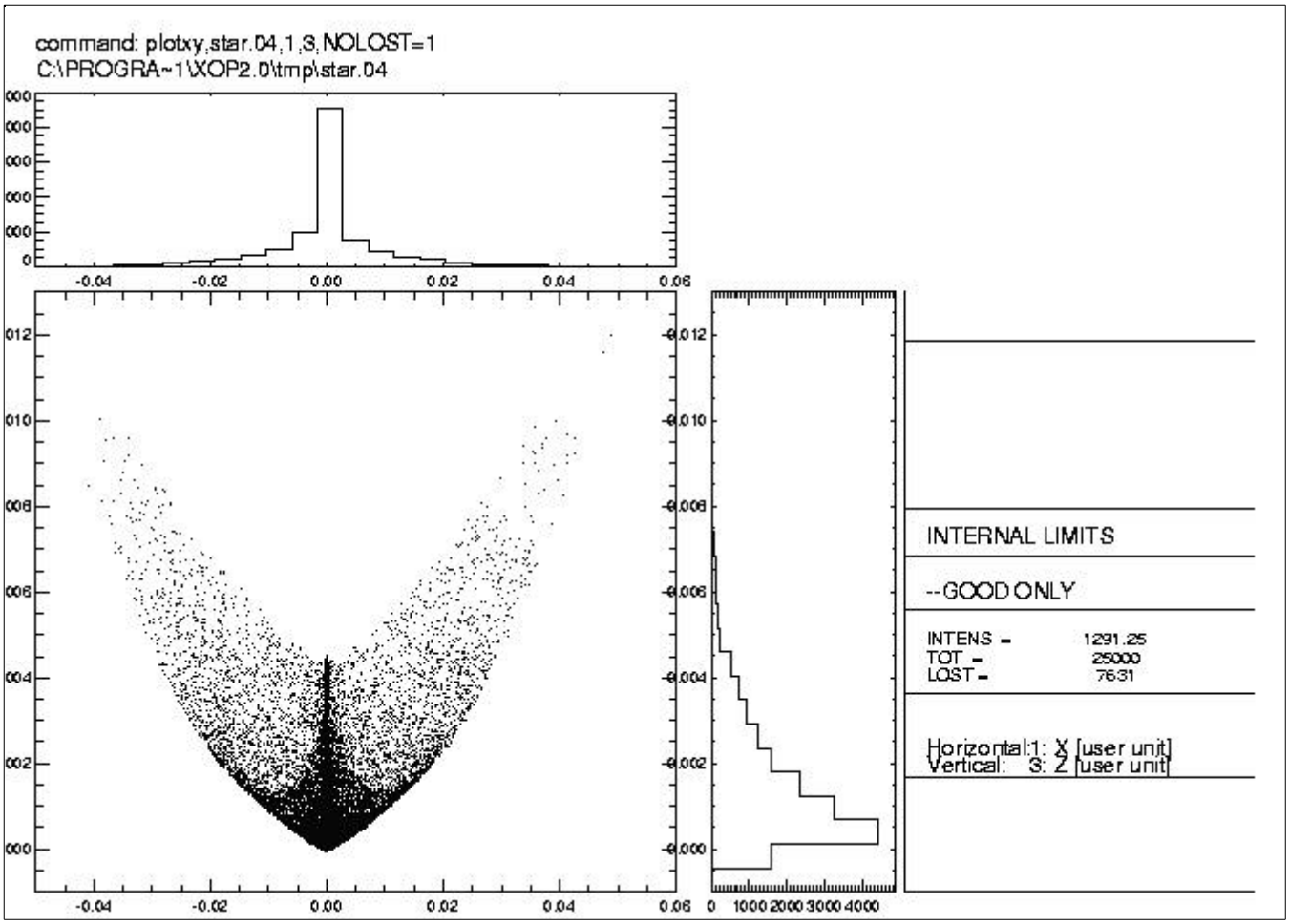

Fig. 9. Image at the focus of an optical system consisting of a parabolic collimator mirror (6.5 m from the source, 4 mrads grazing angle), a pair of flat crystals and a toroidal mirror (20 m from the source, 10 m to the image plane, 4 mrads grazing angle). A point source is used.

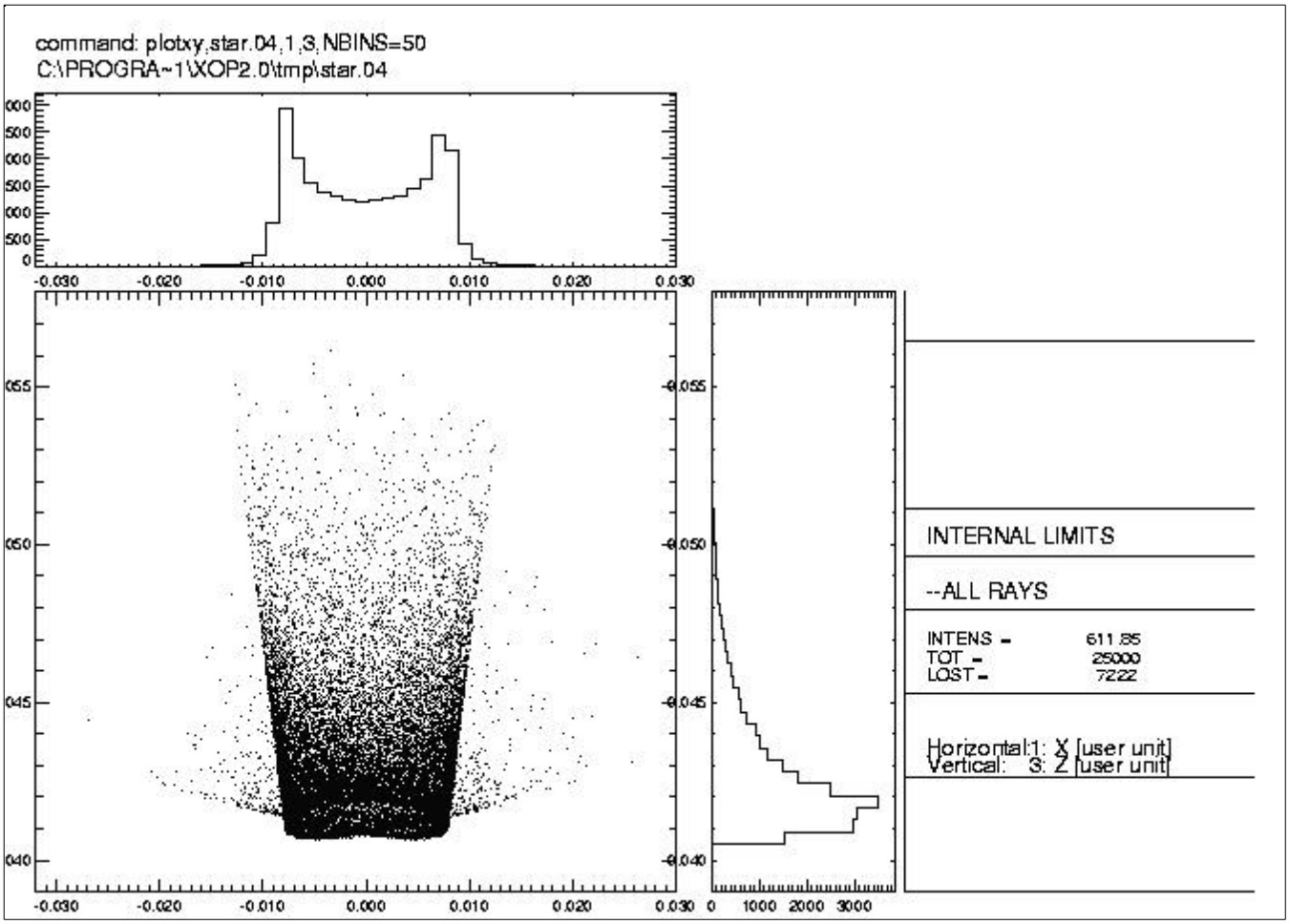

Fig. 10. Image of a point source for the toroidal mirror focusing scheme given in Fig. 9, but with the 2nd crystal C2 rotated by 20 μrads.

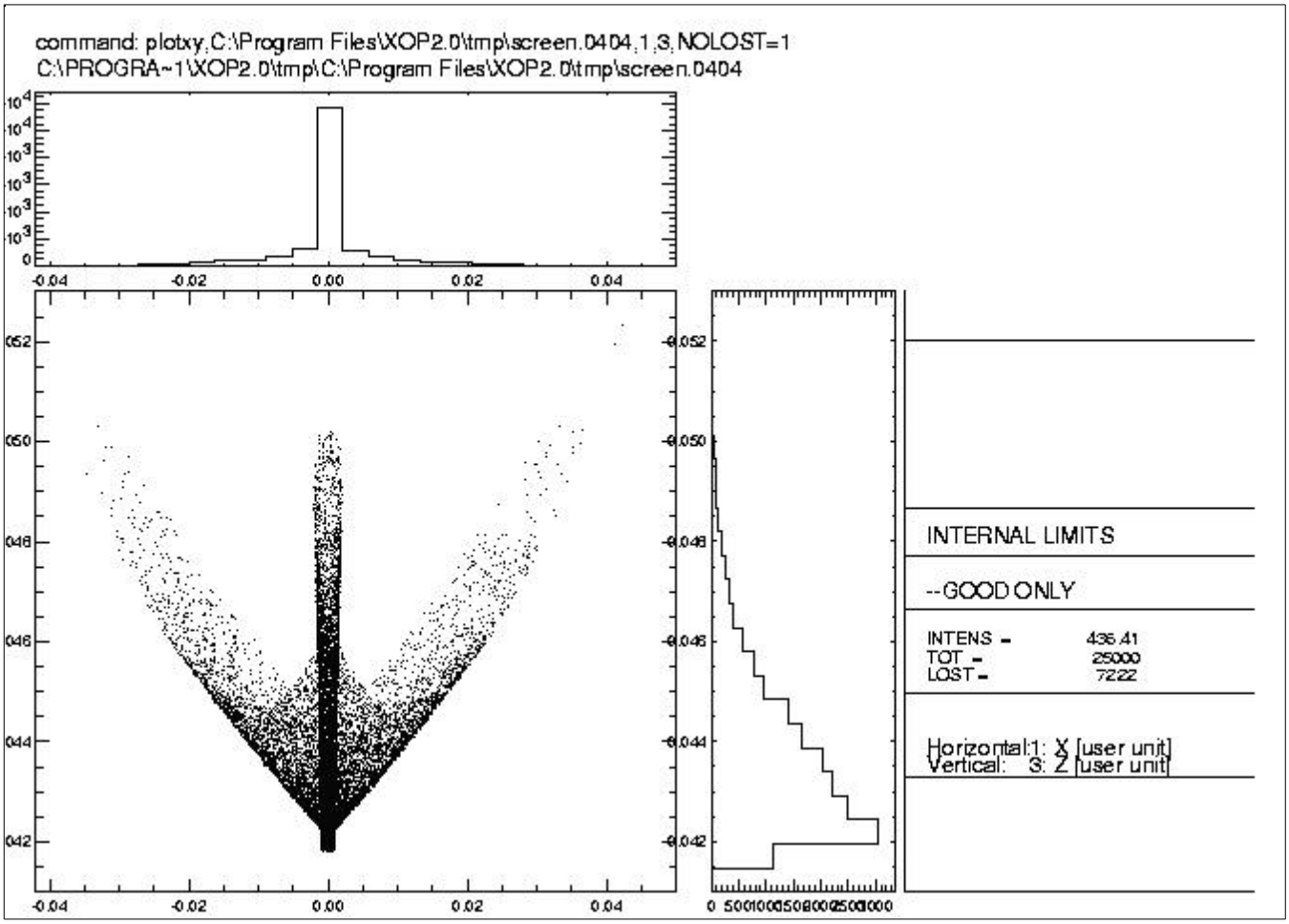

Fig. 11. Image 0.12 m downstream for the toroidal mirror focusing scheme given in Fig. 9 with a 20 μrad rotation of the C2 2nd crystal, as in Fig. 10. Image shown for a point source.

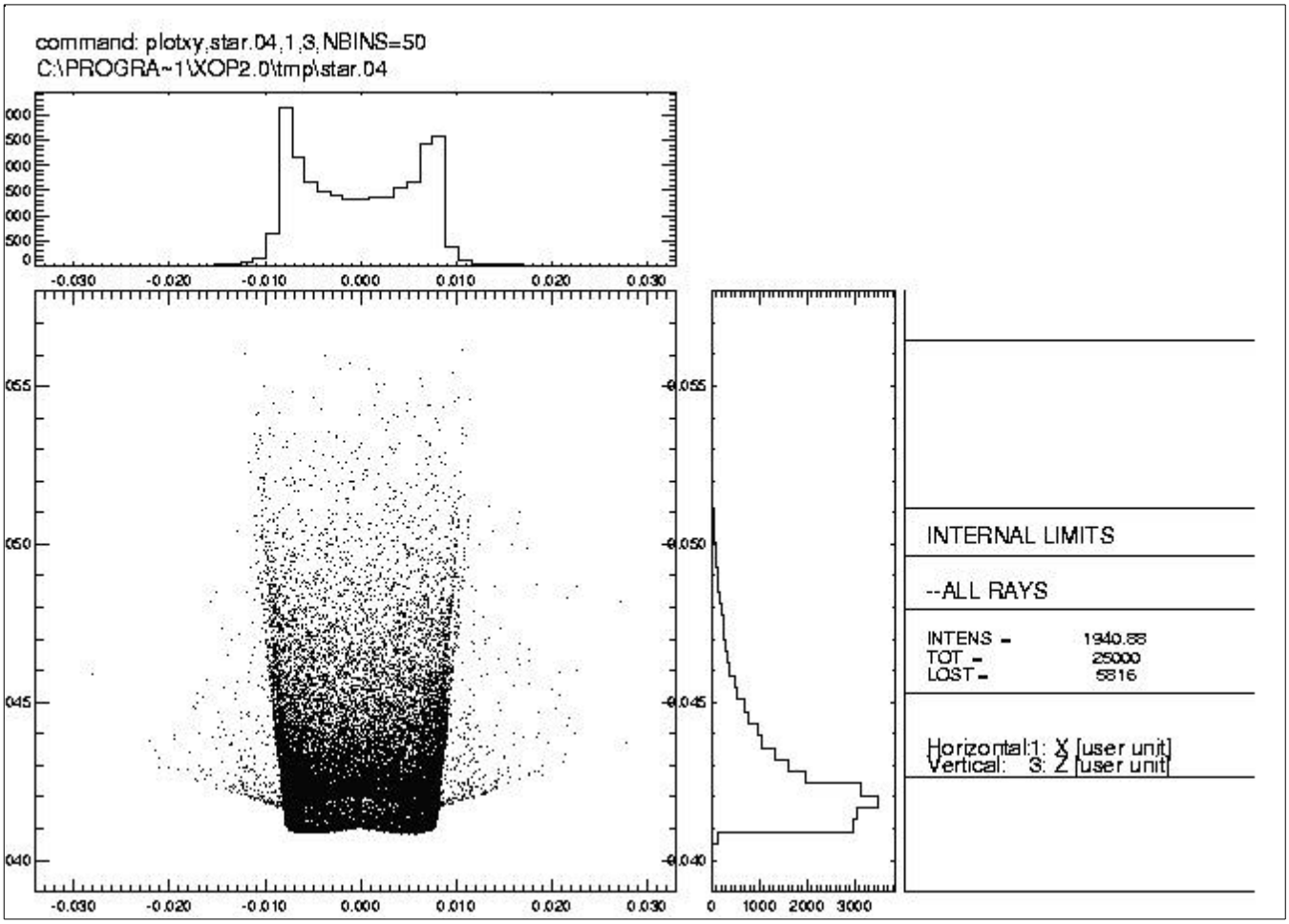

Fig. 12. Image of a point source for the toroidal mirror focusing scheme given in Fig. 9, but with the 1st mirror M1 rotated in pitch by 20 μrads.